Korean J. Chem. Eng., 34(4), 1192-1198 (2017)
DOI: 10.1007/s11814-016-0341-x

pISSN: 0256-1115
eISSN: 1975-7220

Scattering model for tetrapods with cylindrical arms

Seok Kyoo Seo, Hyeonjun Heo, Jeewoo Lim, and Kookheon Char†

The National CRI Center for Intelligent Hybrids
The WCU Program of Chemical Convergence for Energy & Environment
School of Chemical & Biological Engineering, Seoul National University, Seoul 08826, Korea
(*Received 13 August 2016 • accepted 29 November 2016*)

Abstract−A scattering model for regular tetrapods, which are the endoskeleton structure of regular tetrahedrons, is presented. Since a tetrapod, unlike spheres and cylinders, is an anisotropic structure formed by four cylinders branching out from the centroid to the vertices of a tetrahedron, additional symmetry elements and random orientation must be accounted for to develop its scattering model. The scattering function of tetrapods was derived from the modification of the scattering model for cylinders and their structural regularity was simplified. Scattering intensity profiles and pair distance distribution functions were obtained by numerical calculation and compared with the experimental data from small angle X-ray measurements of CdSe tetrapod nanocrystals.

Keywords: Scattering Model, Tetrapod, Nanocrystal, Small Angle X-ray Scattering, Pair Distance Distribution Function

INTRODUCTION

Inorganic nanoparticles or nanocrystals have been studied for various applications due to their unique optical [1] and electrical [2,3] properties, which are different from their properties in the bulk state. Tetrapod nanocrystals, with their distinctive structure consisting of four identical cylindrical arms stretching out at equal angles relative to one another, have been anticipated as a novel class of materials which could facilitate the transport of charge carriers and enhance the area of contact with the surroundings by the virtue of increased surface area [4]. Due to such structural uniqueness, the properties of tetrapods are more strongly affected by their size and shape than the lower-dimensional spheres and rods. Therefore, the geometry of tetrapod nanocrystals should be precisely characterized to define their structure-properties relationship. Furthermore, since the aggregation of nanocrystals obscures the unique properties of individual nanostructures, the dispersion behavior of nanocrystals within matrices should be controlled and characterized. Dimensions and dispersion structure are typically characterized by microscopic methods such as TEM and SEM [4,5], but these methods, by nature, do not provide ensemble characteristics. Therefore, even though the geometry and dispersion structure of nanocrystals are often characterized using such imaging techniques, methods for obtaining ensemble average properties is highly desirable. In this respect, scattering methods have recently been used as a power tool for defining the ensemble average properties of various dispersion systems.

Scattering techniques are extremely valuable for the investigation of both structural geometry as well as ensemble-average spatial distribution of various particles dispersed within matrices because the light scattered off the particles provides structural information of individual particles as well as the correlation between particles. Since the intensity of scattered light is the Fourier transform function of the distance between scattering centers, the scattering intensity needs to be fitted with relevant theoretical models. However, while scattering models for the dispersion properties of structures such as spheres, cylinders, ellipsoids, and hollow spheres, which all have one axisymmetry, have been reported [6,7], similar studies on anisotropic structures, such as tetrapods, which do not have cylindrical symmetry, are scarce.

To deduce theoretical scattering models, the relevant position vectors of the objects of interest should be transformed into the Fourier space. Therefore, the position vectors should be specified in a 3-dimensional coordinate system to account for the volumetric geometry as well as the random orientation. In the case of anisotropic structures, however, the specification of position vector to account for random orientation is extremely difficult using Fourier transform.

We found that, in the case of structurally regular tetrapods, the scattering model can be derived by modifying the cylinder model. Therefore, in this work, we presented the modified cylinder model to take into account the inter-arm correlations of individual tetrapods, followed by the scattering model to account for the random orientation of tetrapods in dispersions. These models were fitted to scattering intensity profiles and pair distance distribution functions by numerical calculations. These functions were then compared with the experimental data from small angle X-ray scattering measurements on CdSe tetrapod dispersions in THF.

SCATTERING MODEL FOR TETRAPODS

1. Scattering Intensity from a Tetrapod

Since a tetrapod is an assembly of four arms, the amplitude of scattered light from a single tetrapod is found by the sum of amplitude

†To whom correspondence should be addressed.
E-mail: khchar@plaza.snu.ac.kr

from each arm (i.e., Debye scattering formula, Eq. (1)). The square of the total amplitude produces the intensity of scattered light. Splitting with n=m, the first term represents the scattering intensities from individual arms and the second term represents the scattering from correlations between a pair of arms [8].

$$A(q)=\sum_{n=1}^{4}A_n(q)\cdot e^{-iqr_n} \tag{1}$$

$$I(q)=\langle|A(q)||A^*(q)|\rangle=\sum_{n=1}^{4}\langle A_n(q)\cdot A_n^*(q)\rangle + \left\langle\sum_{n=1}^{4}\sum_{m\neq n}^{4}A_n(q)\cdot A_m^*(q)\cdot e^{-iqr_{nm}}\right\rangle \tag{2}$$

The angle bracket of Eq. (2) stands for the random orientation, which is the average of all orientations. The scattering amplitudes and intensities from each arm and correlation are not identical because of different orientations and relative positions, although all four arms have the identical dimensions and included angles. However, considering random orientation, the scattering intensity from identical geometric structures should be equal. Correlations from each pair of arms also should show identical scattering profiles because all of the six pairs are isomorphic. Therefore, the scattering intensity of tetrapods is simplified as:

$$I(q)=4\times I_{arm}(q)+6\times I_{Corr}(q) \tag{3}$$

where $I_{arm}(q)$ and $I_{Corr}(q)$ are the intensity of scattered light from an arm and correlation between arms, respectively.

2. Scattering Intensity from a Single Arm

The amplitude of scattered light is calculated by the Fourier transform of position vector with scattering vector, which is given by:

$$A(\mathbf{q})=\int_V e^{-i\mathbf{q}\cdot\mathbf{r}}d\mathbf{r} \tag{4}$$

The position vectors of cylinders are decomposed into a longitudinal and a transverse element in cylindrical coordinate system. Therefore, the scattering amplitude for a cylinder oriented at an angle (θ) from the scattering vector is the product of both contributions [6]:

$$A(q,u)=\int_V e^{-iq\cdot(r_z+r_\perp)}d\mathbf{r}=A_z(q,u)A_\perp(q,u) \tag{5}$$

$$A_z(q,u)=\frac{1}{L}\int_{-L/2}^{L/2}\exp[-iquz]dz=\frac{\sin(quL/2)}{quL/2} \tag{6}$$

$$A_\perp(q,u)=\frac{1}{\pi R^2}\int_0^R\rho\int_0^{2\pi}\exp[-iq\sqrt{1-u^2}\cos(\varphi)\rho]d\varphi d\rho = \frac{2J_1(q\sqrt{1-u^2}R)}{q\sqrt{1-u^2}R} \tag{7}$$

$$A(q,u)=\left[\frac{\sin(quL/2)}{quL/2}\right]\left[\frac{2J_1(q\sqrt{1-u^2}R)}{q\sqrt{1-u^2}R}\right] \tag{8}$$

where and J_1 is the first order Bessel function of the first kind.

The orientation of a cylinder, the direction of the longitudinal element (i.e., director vector), is presented as an angular coordinate (θ, Φ) of the spherical coordinate system. Thus, all the orientations of a cylinder can be considered by integration over all the solid angles in two rotational directions. For the tetrapod, however, these two rotations do not sufficiently describe the random orientation.

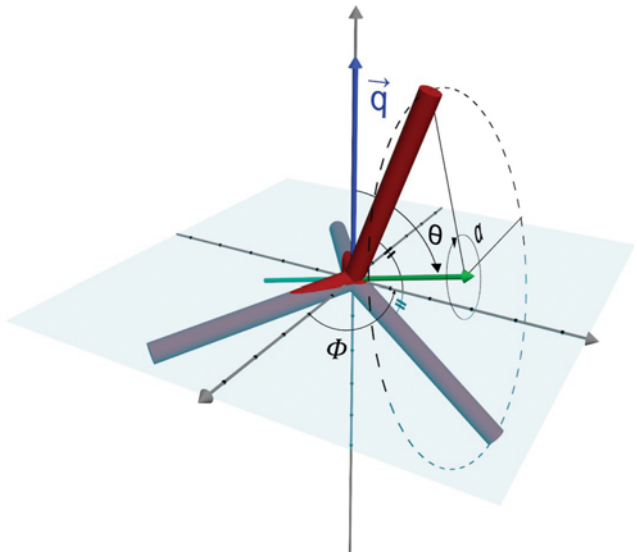

Fig. 1. The rotational directions (θ, Φ, α) of a tetrapod for the random orientation. The bisector (green arrow) of the two arms is the reference of angular coordinate (θ, Φ), which is the axis for the additional rotation (α).

Generally, the number of the degrees of freedom for the rotational movement is three in three-dimensional space, and it is therefore necessary to consider three rotational directions for random orientation. If an object has a rotational symmetry with respect to any angle, also known as axisymmetry, the number of the degree of freedom is decreased with the increase in the number of axisymmetry, like spheres (DOF=0) or cylinders (DOF=2).

Since an anisotropic object, such as a tetrapod (Fig. 1), does not have any axisymmetry, all three rotational directions must be considered for the random orientation. Two of the three rotations correspond to the rotations by polar angle (θ) and azimuthal angle (Φ) in the spherical coordinate, just like the cylinder model. The third is the rotation by the cylindrical angular coordinate (α) about the direction vector of the spherical angular coordinate (θ, Φ) (i.e., green arrow in Fig. 1). The tetrapod has three two-fold rotational symmetry, with the direction vector of a bisector of the angle between two arms being a rotational symmetry axis. Therefore, the direction vector is the reference of angular coordinate (θ, Φ) of the spherical coordinate system. Thus, the orientations of four arms can be presented by θ, Φ, and α in the three-dimensional coordinate system.

At a certain orientation (θ, Φ, α), the dot product of scattering vector ($\vec{\mathbf{q}}$) and position vector ($\vec{\mathbf{r}}_z$) for the longitudinal element of an arm is equal to the vertical element of the $\vec{\mathbf{r}}_z$ (Fig. 2). From the side view (Fig. 2(b)), the vertical element of the vector $\vec{\mathbf{r}}_z$ is deduced to $|r|(\cos A\cos\theta+\sin A\sin\theta\cos\alpha)$, implying that the angle between scattering vector ($\vec{\mathbf{q}}$) and position vector ($\vec{\mathbf{r}}_z$) is $\cos^{-1}(\cos A\cos\theta+\sin A\sin\theta\cos\alpha)$. Therefore, in Eq. (6) would be replaced by $\cos A\cos\theta+\sin A\sin\theta\cos\alpha$ for the longitudinal contribution of the arm. The transverse contribution, however, cannot be derived in this way because the angle of φ in Eq. (7) varies with the rotation by the angle

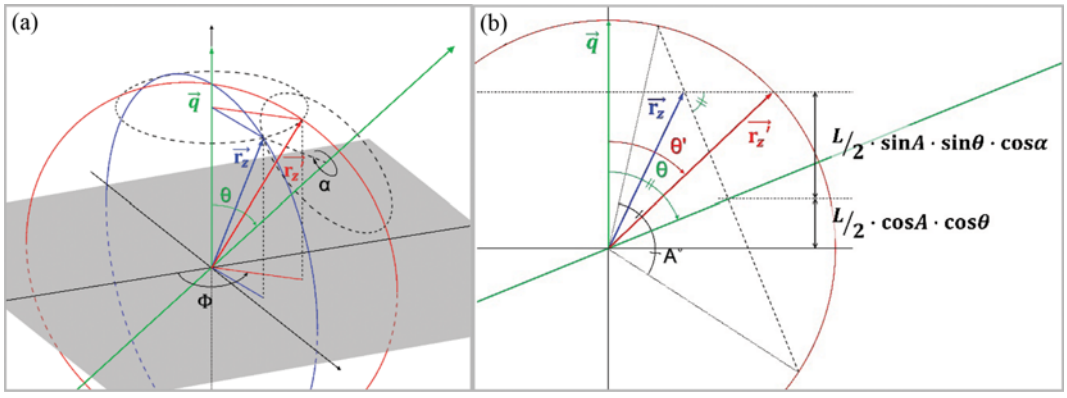

Fig. 2. Three-dimensional scheme (a) to illustrate the orientation (θ, Φ, α) and its side view (b). The longitudinal element of an arm oriented at (θ, Φ, α) is the blue vector ($\vec{r}_z$), which is out of the red plane (a). However, the height of $\vec{r}_z$ is the same as the height $\vec{r}'_z$ which is L/2cosAcosθ+sinAsinθcosα (b). An angle of A is the half of the tetrahedral angle (i.e., 109.5/2°).

of α.

Nevertheless, Eq. (7) can be used for the computation of the transverse contribution of arms by replacing u with cosAcosθ+sinAsinθ cosα, as was done with longitudinal contribution, because the dot products of cylinders oriented at vector ($\vec{r}_z$) and ($\vec{r}'_z$) with the scattering vector ($\vec{q}$) are identical. It means that there is the orientation of (θ', Φ, α=n π/2) corresponding to the orientation of (θ, Φ, $\alpha\neq$n π/2) and the average of all the orientation from a single arm does not change. Therefore, the scattering amplitude from each is are given by:

$$A_n(q,\theta,\alpha)=\left[\frac{\sin(qu_nL/2)}{qu_nL/2}\right]\left[\frac{2J_1(q\sqrt{1-u_n^2}R)}{q\sqrt{1-u_n^2}R}\right] \tag{9}$$

$$\begin{aligned}
u_1&=\cos A\cos\theta+\sin A\sin\theta\cos\alpha\\
u_2&=\cos A\cos(\theta+\pi)+\sin A\sin(\theta+\pi)\cos\left(-\alpha+\frac{\pi}{2}\right)\\
&=-\cos A\cos\theta-\sin A\sin\theta\sin\alpha\\
u_3&=\cos A\cos\theta+\sin A\sin\theta\cos(\alpha+\pi)\\
&=\cos A\cos\theta-\sin A\sin\theta\cos\alpha\\
u_4&=\cos A\cos(\theta+\pi)+\sin A\sin(\theta+\pi)\cos\left(-\alpha+\frac{3\pi}{2}\right)\\
&=-\cos A\cos\theta+\sin A\sin\theta\sin\alpha
\end{aligned} \tag{10}$$

where the negative in front of α is respect to the rotational direction. Numbers of arms (n=1, 2, 3 and 4) in a tetrapod are assigned in the clockwise fashion.

3. Scattering Intensity from the Correlations of a Pair of Arms

For the scattering intensity from the correlation between two arms, different two arms of a tetrapod should be considered, while the scattering intensity from an arm needs an arm of a tetrapod. From the second term of Eq. (2), scattering intensity from the correlation of any pair of arms is obtained by expansion of sigma. The function is given by:

$$\begin{aligned}
&\langle A_m(q,\theta,\alpha)\cdot A_n^*(q,\theta,\alpha)\cdot e^{-iq\mathbf{r}_{mn}}\rangle\\
&\quad+\langle A_n(q,\theta,\alpha)\cdot A_m^*(q,\theta,\alpha)\cdot e^{-iq\mathbf{r}_{nm}}\rangle
\end{aligned} \tag{11}$$

where the vector **r** represents the position of arms and the subscripts m and n are the arm numbers which are different. The direction of the vector **r** is the same as the corresponding u and the magnitude of the vector **r** is L/2. Since the amplitudes of arms are real functions, the conjugate complexes are identical to the original one. Therefore, the scattering intensity from the correlations would be simplified to the cosine function:

$$\begin{aligned}
&\langle A_m(q,\theta,\alpha)\cdot A_n^*(q,\theta,\alpha)\cdot e^{-iq\mathbf{r}_{mn}}\rangle\\
&\quad+\langle A_n(q,\theta,\alpha)\cdot A_m^*(q,\theta,\alpha)\cdot e^{-iq\mathbf{r}_{nm}}\rangle\\
&=2\left\langle A_m(q,\theta,\alpha)\cdot A_n(q,\theta,\alpha)\cdot\left(\frac{e^{-iq\mathbf{r}_{mn}}+e^{iq\mathbf{r}_{mn}}}{2}\right)\right\rangle\\
&=2\langle A_m(q,\theta,\alpha)\cdot A_n(q,\theta,\alpha)\cdot\cos(q\cdot L/2\cdot(u_m-u_n))\rangle
\end{aligned} \tag{12}$$

Finally, by substituting Eq. (9) and (12) into Eq. (3), the scattering intensity from a tetrapod is presented by Eq. (13) (with n, m=1-4, n≠m):

$$\begin{aligned}
I(q)=&\frac{1}{\pi^2}\int_0^{2\pi}\int_0^{\pi}\int_0^{\pi}\left\{\left[\frac{\sin(qu_nL/2)}{qu_nL/2}\right]\left[\frac{2J_1(q\sqrt{1-u_n^2}R)}{q\sqrt{1-u_n^2}R}\right]\right\}^2\sin\theta\,d\alpha\,d\theta\,d\phi\\
&+\frac{3}{\pi^2}\int_0^{2\pi}\int_0^{\pi}\int_0^{\pi}\left[\frac{\sin(qu_mL/2)}{qu_mL/2}\right]\left[\frac{\sin(qu_nL/2)}{qu_nL/2}\right]\\
&\times\left[\frac{2J_1(q\sqrt{1-u_m^2}R)}{q\sqrt{1-u_m^2}R}\right]\left[\frac{2J_1(q\sqrt{1-u_n^2}R)}{q\sqrt{1-u_n^2}R}\right]\cos(q(u_m-u_n)\\
&\cdot L/2)\sin\theta\,d\alpha\,d\theta\,d\varphi
\end{aligned} \tag{13}$$

SMALL ANGLE X-RAY SCATTERING EXPERIMENTS OF TETRAPOD NANOCRYSTALS

The experimental scattering intensity profile of tetrapod dispersions was obtained by small angle X-ray scattering (SAXS) measurements and was used to test the validity of our model. Well-defined CdSe tetrapod nanocrystals were synthesized by the continuous precursor injection (CPI) method developed by our group [5]. Tetrapods with three different arm lengths (~40, ~55, ~70 nm), all with the identical arm radius (~3 nm), were used for the SAXS experiments.

The tetrapods were dispersed in THF at different concentrations. To obtain the scattering intensity from a single tetrapod, tetrapods

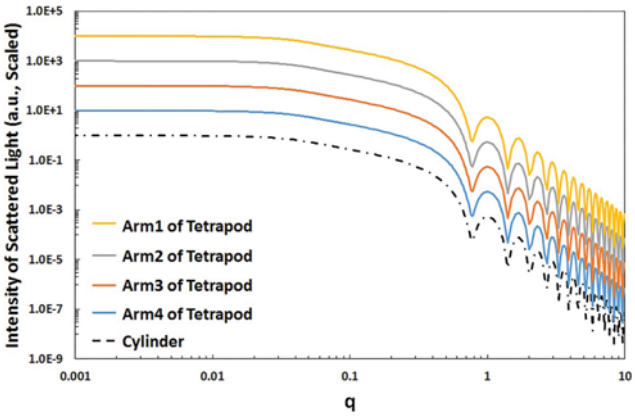

Fig. 3. Numerical results of the scattering model for the arms of tetrapods and individual cylinders. All the numerical results of the scattering intensity show the same scattering profiles with the same dimensions (i.e., L=100 & R=5).

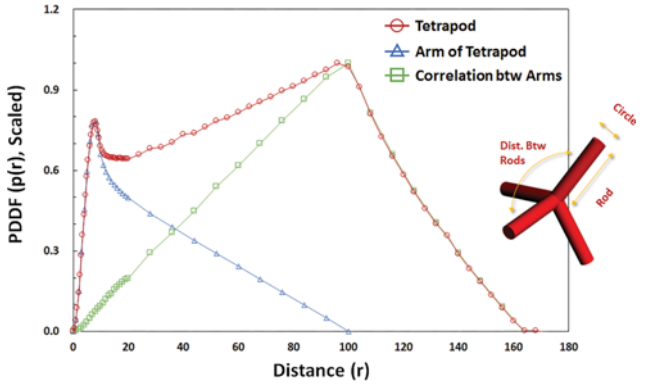

Fig. 5. PDDF of a tetrapod (red), the correlation of arms (green) and the arm of a tetrapod (blue) with R=5 and L=100. The distances at the two peaks and the endpoint in PDDF correspond to the radius and length of arms and the maximum distance between arms.

were dispersed in THF at a highly dilute concentration (0.1 mg/ml). Dispersions at other concentrations (3, 10, 30 mg/ml) were prepared to confirm the critical concentration.

As the range of distance within tetrapod nanocrystals in real space is 6-120 nm, 9A beam line (U-SAXS) of Pohang Accelerator Laboratory, which includes the relevant q-range of 0.005-0.11 $Å^{-1}$, was used. The scattering data at 11.07 keV and 19.95 keV were merged with minimum deviation in the overlap region.

The results from the SAXS measurements and the model proposed in the present study were compared in terms of scattering intensity profiles and the pair distance distribution functions. The pair distance distribution function is produced by the inverse Fourier transform of the scattering intensity profile, which is possible numerically but not analytically. For the inverse Fourier transform, we used the commercial software package (PCG software package) for the indirect Fourier transform method.

RESULTS AND DISCUSSION

1. Validity of the Additional Rotation α

The scattering model for tetrapods was facilitated by adding the rotation about the direction vector of angular coordinates. None-

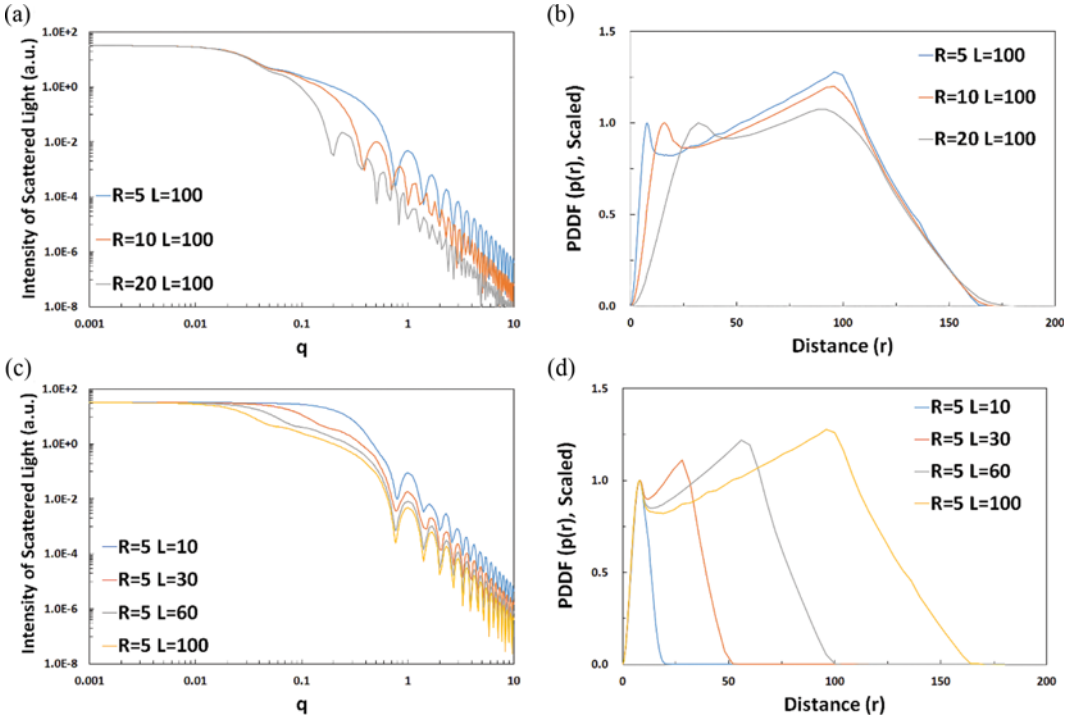

Fig. 4. Numerical results of the scattering model for tetrapods. Scattering intensity profiles (a) & (c) and PDDFs (b) & (d) of tetrapods with different arm radii (a) & (b) and arm lengths (c) & (d).

theless, the scattering intensity from a single arm should not be changed because the added rotation does not lead to the change of volume.

However, it is hard to demonstrate mathematically that the scattering intensities from the cylinder model and the arm of the tetrapod model are identical because the angle of α is present both in the denominator and the first-order Bessel function. Therefore, the scattering intensities from an arm of a tetrapod (with α, solid lines in Fig. 3) and a cylinder (without α, dashed line in Fig. 3) were compared by numerical calculations and demonstrated to have the same scattering intensity profiles in Fig. 3. The lines in Fig. 3 are vertically shifted to compare each other easily.

2. Scattering Intensity and PDDF of the Model for Tetrapods

As the total scattering intensity from tetrapods is obtained by the summation of intensity from each arm and correlation, the profiles of tetrapods would show the characteristics of both contributions (Fig. 4). The profile in the plateau region is almost the same with the profile of cylinders and thus corresponds to the contribution from the cylindrical arms. It may therefore be assumed that the shoulder at the end of the plateau region originates from the correlations between the arms. It may also be assumed that the position of the scattering shoulder would not change with the arm radius but rather

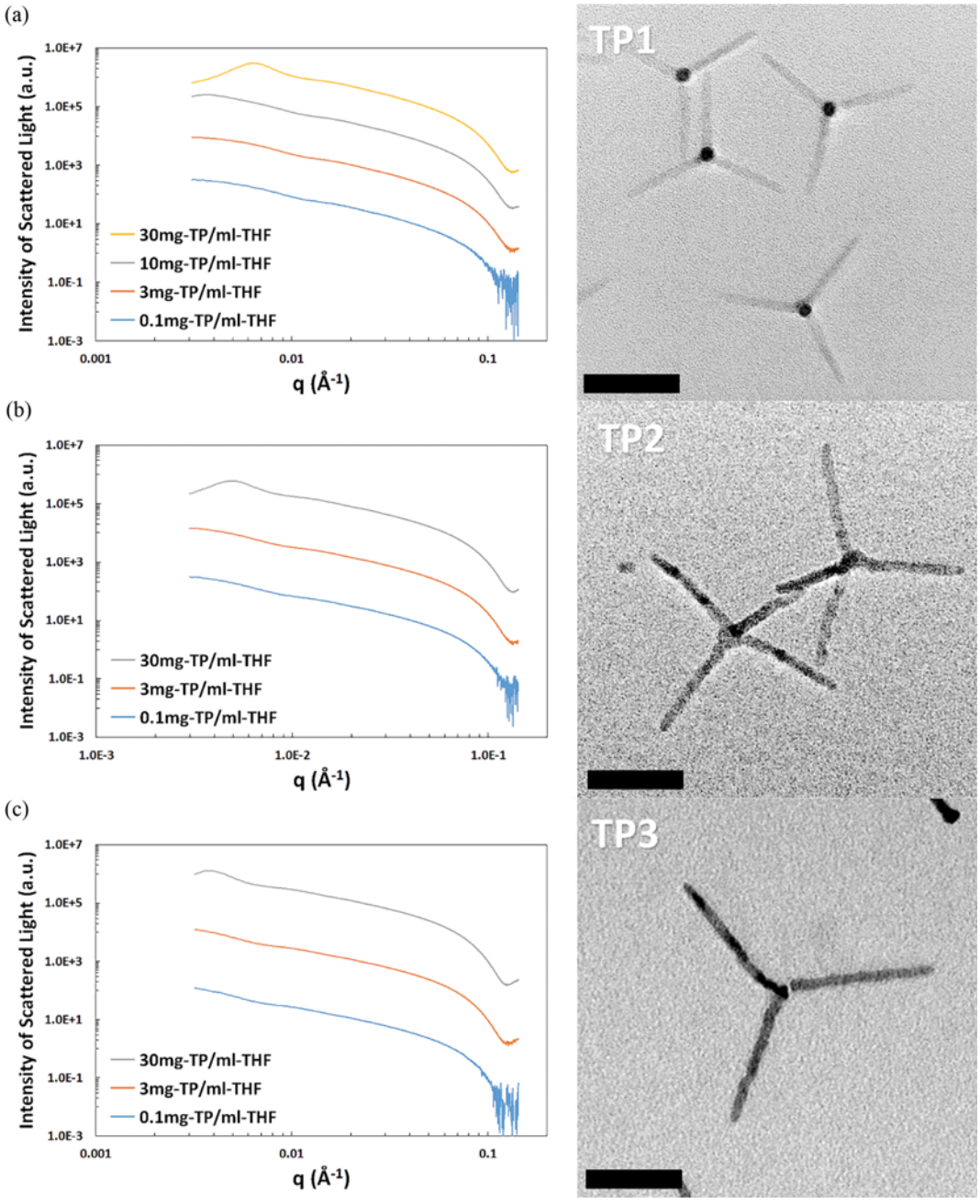

Fig. 6. TEM images and scattering intensity profiles of tetrapod nanocrystals. Radii of tetrapods tested are all around 3 nm and the arm lengths are 40 (a, TP1), 55 (a, TP2) and 70 nm (a, TP3), respectively. Scale bar=50 nm.

with the arm length. The small plateau region just after the shoulder is not the Guinier region of cylinders, which comes from the lower q range, but the first fringe of the scattering intensity profile from correlations. After that, however, the scattering intensity from the correlations decays rapidly and has negligible effect on the total scattering intensity.

The pair distance distribution function (PDDF) of tetrapods is the accumulation of the PDDPs of cylinders and correlations (Fig. 5). Each function can be obtained by inverse Fourier transform of intensity of scattered light from an arm ($I_{arm}(q)$) and a correlation between arms ($I_{Corr}(q)$) in Eq. (13), respectively. For the PDDF of cylinders, there is, sequentially, a peak for the radial distance and a straight line for the vertical distance of a cylinder body. For the correlation, as in the population of distance between two lines at a given angle, the pair distance distribution function increases through the length of the line and decreases up to the maximum distance between two lines. The PDDF of tetrapods has the features of both cylinders and correlations and thus suitably describes the structural properties of tetrapods.

3. Results from Small Angle X-ray Scattering Measurements

Small angle X-ray scattering (SAXS) experiments were performed for tetrapod solutions in THF with different concentrations (0.1, 3, 10, and 30 mg/ml; 10 mg/ml is only for L=40 nm, Fig. 6). The lowest concentration (0.1 mg/ml) was prepared for mimicking the dilute concentration in which inter-particle correlations are almost negligible. Technically, scattering from a single particle requires infinitely dilute concentration, which is practically impossible. However, if there is no interparticle correlation effect in the relevant q-range, the scatting intensity can be treated by the form factor of a single object. Our observations show that there is no correlation in the low q-range up to a concentration of 3 mg/ml, and from the concentration of 10 mg/ml and higher, the signals of interparticle correlations begin to emerge in the low q range. Therefore, we used the scattering intensity from 0.1 mg/ml solution as the form factor of a tetrapod. Because there are small fluctuations in the scattering intensity at 0.1 mg/ml, this profile is interpolated by the binominal smoothing process. The structure factors of tetrapods with L=40 nm are produced by dividing the scattering intensity with the form factor and are presented in Fig. 7. These structure factors would

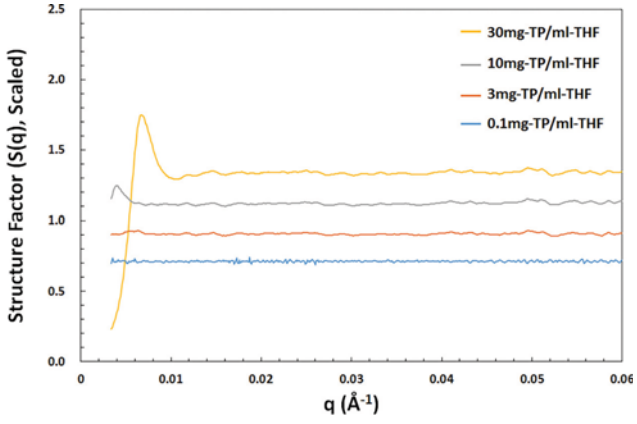

Fig. 7. The structure factors of tetrapod nanocrystals (R=3 and L=40 nm) with different concentration.

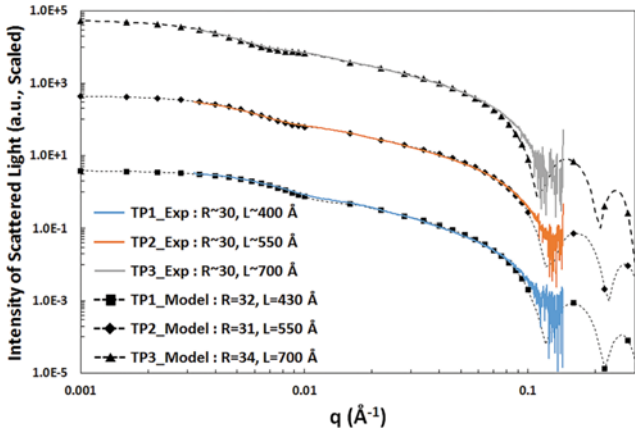

Fig. 8. The form factors of tetrapod nano-objects obtained from the SAXS experiments (solid line) along with the fit to the model (symbols). The form factors from the SAXS experiments were obtained from the measurements in dilute solution (0.1 mg-TP/ml-THF) of tetrapod nanocrystals.

inform the average distance between tetrapods. The structure factor for 0.1 mg/ml (Fig. 7, blue line) is the ratio between the raw and smoothed data, which shows the degree of fluctuations.

The form factors obtained from the SAXS measurements were fitted with the scattering model presented in this paper (Fig. 8). All the experiment results are in relatively good agreement with the profiles from the model except at the high q range. In this region, of course there are some fluctuations due to the high signal to noise ratio, and the experimental scattering intensities are higher than that predicted by our model. This deviation is presumed to originate from either the polydispersity of nanocrystals or the geometry of the arm ends. While our scattering model assumed that the tetrapods are monodisperse in size and that their arms are the cyl-

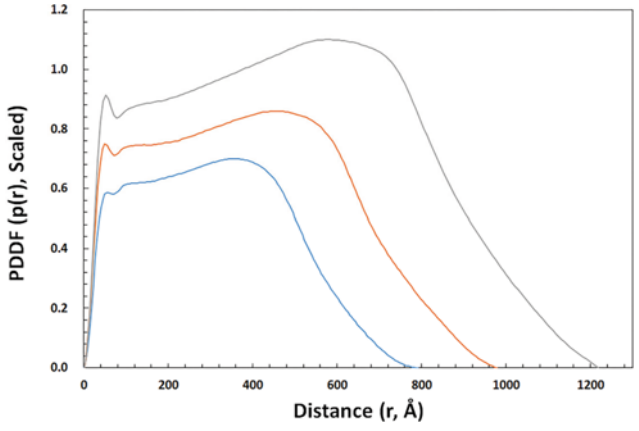

Fig. 9. Pair distance distribution functions (PDDF) of TPs. Form factors obtained from the SAXS measurements of TPs in dilute solutions are transformed into PDDFs by indirect Fourier transform, which shows similar characteristics with the PDDFs of the current scattering model for tetrapods. Distances at the peak, the inflection point, and the endpoint correspond to the radius, length of arms, and the maximum distance between arms in tetrapods, respectively.

inders with flat ends, the real tetrapod nanocrystals are not strictly monodisperse and the geometry at arm ends is closer to hemispheres or hemi-ellipsoids than the truncated cylinders.

To figure out the difference in real space, the PDDF of SAXS measurements were obtained by the inverse Fourier transform (Fig. 9). The profiles of the PDDF have the same characteristics as our model. The peak corresponding to the radius of a tetrapod and the inflection corresponding to the correlations of arms appear in sequence, and the profiles end at the distance corresponding to the maximum distance between arms. However, compared to our scattering model, all these characteristics are smeared. Either the presence of size polydispersity or the variations in radius within each arm caused by hemispherical or hemi-ellipsoidal ends may result in such smearing. Since, however, the volume of round ends is extremely small with respect to the total volume of a tetrapod, the difference may be attributed exclusively to the size polydispersity of the tetrapods.

Since the small difference between the scattering intensities of SAXS experiments and our model, which appears only in the high q range, could be attributed to the innate polydispersity in the arm lengths of real CdSe tetrapods, we believe that our scattering model for the tetrapods, and the general approach towards providing scattering models for anisotropic structures it puts forward, are acceptable.

4. Model Expansion to Regular Multi-Pod Structures

In this work, we demonstrate that scattering functions of tetrapods with identical arms and included angles can be established despite the anisotropic structure. Likewise, scattering functions of multipod structures with identical arms may be approached in a similar manner, while accounting for the presence of more than one type of included angle.

For example, an octopod [9-11], which is a multipod with eight arms branching out from the vertices of a regular hexahedron core, has 28 two-arm combinations. Among them, 12 combinations with neighboring arms have an included angle of 70.5°, another 12 combinations with face diagonal arms have an angle of 109.5°, and the remaining four combinations with space diagonal arms an angle of 180°. As the rotation about the line connecting the center of top and bottom faces of hexahedron, all orientations can be covered by three kinds of correlations. Therefore, the scattering amplitude from a multipod with eight arms is determined by the scattering amplitude of the arms and the three types of arm-arm correlations. Likewise, the hexapod, which is formed by connecting the centroid of an octahedron to its vertices, can be described using two types of arm-arm correlations (90° and 180°).

Thus, for the anisotropic multipods with rotational symmetry, the position of arms would be described by the rotation about symmetry axes, and scattering intensity can be obtained by accounting for the nature of included angles.

Note that the overlapped volume at the centroid is ignored in this model. For tetrapods, due to the large included angle, the overlapped volume is negligible. However, it is impossible to disregard the overlapped volume if the lengths of arms are short relative to the radius or if the angles between arms are small. In these cases, the relevant object should be placed and all scattering amplitudes must be considered individually.

CONCLUSION

A scattering model for tetrapods is presented and compared with the actual SAXS data obtained from CdSe tetrapods in solution. To account for the random orientation of anisotropic tetrapods, additional rotations about the axes of rotational symmetry were introduced. By numerical calculations, the scattering intensity profile and the PDDF of tetrapods was presented, and it was shown that the model successfully described the geometry of tetrapods.

To obtain the form factor of tetrapods experimentally, SAXS for dilute CdSe tetrapod solutions in THF (0.1 mg/ml) were measured and the critical concentration range was determined by comparison with solutions with higher concentrations. The scattering intensity, as well as the PDDF reduced by the inverse Fourier transform method, was compared with our theoretical model. Although there is a slight difference between our model and the experimental data in the high q range, overall profiles of the scattering intensity and the PDDF from SAXS measurements showed the characteristics of tetrapods and fit well to the model. From these results, we demonstrate that the scattering model presented in this study is acceptable.

Our current approach can also be extended to other multipods formed by connecting the centroid to the vertices of regular polyhedra. Increasing the number of arms would complicate the calculations due to the higher number of correlations which must be considered, but the overall model presented here will be applicable.

REFERENCES

1. N. C. Greenham, X. Peng and A. P. Alivisatos, *Phys. Rev. B*, **54**, 17628 (1996).
2. P. Peng, D. J. Milliron, S. M. Hughes, J. C. Johnson, A. P. Alivisatos and R. J. Saykally, *Nano Lett.*, **5**, 1809 (2005).
3. S. Malkmus, S. Kudera, L. Manna, W. J. Parak and M. J. Braun, *J. Phys. Chem. B.*, **110**, 17334 (2006).
4. J. Lim, W. K. Bae, K. U. Park, L. zur Borg, R. Zentel, S. Lee and K. Char, *Chem. Mater.*, **25**, 1443 (2013).
5. J. Lim, L. zur Borg, S. Dolezel, F. Schmid, K. Char and R. Zentel, *Macromol. Rapid. Comm.*, **35**, 1685 (2014).
6. Guinier and Fournet, *Small Angle X-Ray Scattering*, Wiley, New York (1955).
7. J. S. Pedersen, *Adv. Colloid Interface Sci.*, **70**, 171 (1997).
8. R. J. Roe, *Methods of x-ray and neutron scattering in polymer science*, Oxford University Press (2000).
9. Z. Zhao, Z. Zhou, J. Bao, Z. Wang, J. Hu, X. Chi, K. Ni, R. Wang, X. Chen, Z. Chen and J. Gao, *NATURE COMMUNICATIONS*, **4**, Article number: 2266 (2013).
10. K. Miszta, J. de Graaf, G. Bertoni, D. Dorfs, R. Brescia, S. Marras, L. Ceseracciu, R. Cingolani, R. van Roij, M. Dijkstra and L. Manna, *NATURE MATERIALS*, **10**, 872 (2011).
11. E. Conca, M. Aresti, M. Saba, M. F. Casula, F. Quochi, G. Mula, D. Loche, M. R. Kim, L. Manna, A. Corrias, A. Mura and G. Bongiovanni, *Nanoscale*, **6**, 2238 (2014).